Phobos has been excavated and fragmented by impacts. The mean excavation depth was estimated to be hundreds of meters (*2*). Material ejected from Phobos has remained in the gravitational potential well of Mars, and a significant fraction was later recaptured to form a regolith on the satellite (*23*). The fact that Phobos shows neither albedo nor color variation down to a resolution of 200 m (*3*) supports this conclusion. If material in the interior were excavated and then darkened by exogenous processes similar to those on Earth's moon, we would see bright (fresh) and dark (old) features like the rays on the lunar surface (*24*).

Is the surface composition of Phobos, Ceres, or any other carbonaceous body really the same as the bulk composition? Is it possible that the carbonaceous material is merely a superficial deposit, perhaps accreted from meteoritic or cometary debris? Morrison (*25*) reviewed the size and density of Ceres and concluded that the low density of this asteroid (~ 2.5 g/cm^3) is consistent with a bulk composition similar to that of carbonaceous chondrites. Laboratory photometric studies of returned lunar samples show no evidence that the meteoritic component controls the bulk spectral reflectivity (*26*).

Our identification of a carbonaceous chondritic composition for Phobos is consistent with the implications of a recent mass estimate for the satellite based on the perturbations on the orbit of Viking 1 by Phobos, during a series of close encounters. This mass estimate yields a density of 2.0 ± 0.6 g/cm^3 (*27*). Such a low density is consistent with that of type 1 or type 2 carbonaceous chondrites, but it definitely rules out basalts which have densities close to 3 g/cm^3. Our reflectance data and the low-density value have eliminated the possibility that Phobos originated from a parent body large enough to have melted and differentiated to form basalts. Rasool and Le Sergeant (*28*) found that the relative abundance and total amounts of noble gases on Mars, measured by Viking, can best be explained if the outer layers of Mars were made of material similar to that of ordinary chondrites (type LL) as suggested by Anders (*29*) rather than carbonaceous chondrites as assumed by a number of investigators in recent years. Both our work and (*28*) point to different modes of origin for Mars and Phobos.

In order to choose among other possible origins, we must determine precisely which type of carbonaceous chondrite material Phobos most resembles.

If Phobos is made of the most primitive type carbonaceous chondrite material (C1), as its low density suggests, then the satellite is almost certainly a captured body which formed in the asteroid belt, since volatile-rich C1 materials probably did not form as close to the sun as Mars (*30*). The uncertainty in the density value still allows the possibility that Phobos is made of C2 carbonaceous chondrite material, as C2 materials have densities in the range 2.5 to 2.9 g/cm^3 (*31*); C2 material has volatile contents between those of C1 and C3 materials. Type 1 carbonaceous chondrites contain no chondrules but are so classed because they are chemically and mineralogically similar to the chondrule-bearing stones of the same type; type 2 carbonaceous chondrites contain chondrules. Practically all investigators have accepted the idea that chondrules were once molten drops. This hypothesis requires a high temperature and a liquid state of the meteoritic material at one stage of its development. Consequently, a high-temperature origin with some dehydration and reduction but not differentiation still remains a possible interpretation. Refined analyses of our spectral data for secondary features may enable us to test the possibility that Phobos is indeed made of C1 material.

KEVIN D. PANG
Planetary Science Institute,
Pasadena, California 91101
JAMES B. POLLACK
NASA Ames Research Center,
Moffett Field, California 94035
JOSEPH VEVERKA
Laboratory for Planetary Studies,
Cornell University,
Ithaca, New York 14853
ARTHUR L. LANE, JOSEPH M. AJELLO
Jet Propulsion Laboratory,
California Institute of Technology,
Pasadena 91103

References and Notes

1. B. H. Zellner and R. C. Capen, *Icarus* **23**, 437 (1974).
2. J. B. Pollack, J. Veverka, M. Noland, C. Sagan, T. C. Duxbury, C. H. Acton, Jr., G. H. Born, W. K. Hartmann, B. A. Smith, *J. Geophys. Res.* **78**, 4313 (1973).
3. J. Veverka, *Sci. Am.* **236**, 30 (February 1977).
4. J. A. Wood, in *The Dusty Universe*, G. B. Field and A. G. W. Cameron, Eds. (Watson, New York, 1973), pp. 245–266.
5. C. A. Barth, C. W. Hord, A. I. Stewart, A. L. Lane, *Science* **175**, 309 (1972).
6. K. D. Pang and J. M. Ajello, *Icarus* **30**, 63 (1977).
7. M. Noland and J. Veverka, *ibid.* **28**, 405 (1976).
8. A. L. Broadfoot, *Astrophys. J.* **173**, 681 (1972).
9. R. C. Bohlin, D. Frimout, C. F. Lillie, *Astron. Astrophys.* **30**, 127 (1974).
10. C. F. Lillie, R. C. Bohlin, M. R. Molnar, C. A. Barth, A. L. Lane, *Science* **175**, 321 (1972).
11. J. B. Pollack, J. Veverka, K. Pang, D. Colburn, A. L. Lane, J. M. Ajello, *Science* **199**, 66 (1978).
12. B. H. Zellner, personal communication.
13. R. L. Lucke, R. C. Henry, W. G. Fastie, *Astron. J.* **81**, 1162 (1976); A. P. Lane and W. M. Irvine, *ibid.* **78**, 267 (1973).
14. C. R. Chapman, T. B. McCord, T. V. Johnson, *ibid.*, p. 126.
15. D. Morrison, *Icarus* **31**, 185 (1977).
16. J. Caldwell, *ibid.* **25**, 384 (1975).
17. C. R. Chapman, D. Morrison, B. Zellner, *ibid.*, p. 104.
18. C. R. Chapman and J. W. Salisbury, *ibid.* **19**, 507 (1973); T. B. McCord and M. J. Gaffey, *Science* **186**, 352 (1974); T. V. Johnson, D. L. Matson, G. J. Veeder, S. J. Loer, *Astrophys. J.* **197**, 527 (1975).
19. T. V. Johnson and F. P. Fanale, *J. Geophys. Res.* **78**, 8507 (1973).
20. M. J. Gaffey, *ibid.* **81**, 905 (1976).
21. P. J. Foster and C. R. Howarth, *Carbon* **6**, 719 (1968).
22. D. R. Huffman, in *Solid State Astrophysics*, N. C. Wickramasinghe and D. J. Morgan, Eds. (Reidel, Hingham, Mass., 1976), pp. 191–200.
23. S. Soter, *Cornell Univ. Center Radiophys. Space Res. Rep. 462* (1971).
24. W. Cassidy and B. Hapke, *Icarus* **25**, 371 (1975).
25. D. Morrison, *Geophys. Res. Lett.* **3**, 701 (1976).
26. J. R. Adams and T. B. McCord, in *Proceedings of the 2nd Lunar Science Conference*, A. A. Levinson, Ed. (MIT Press, Cambridge, Mass., 1971), pp. 2183–2195.
27. R. H. Tolson *et al.*, *Science* **199**, 61 (1978).
28. S. I. Rasool and L. Le Sergeant, *Nature (London)* **226**, 822 (1977).
29. E. Anders, *Annu. Rev. Astron. Astrophys.* **9**, 1 (1971).
30. J. S. Lewis, *Earth Planet. Sci. Lett.* **15**, 286 (1972).
31. B. Mason, *Meteorites* (Wiley, New York, 1962).
32. Planetary Science Institute contribution No. 82. Funds for this research were provided by NASA. We acknowledge the support of the Mariner 9 UVS and Viking lander imaging teams.

20 May 1977; revised 22 August 1977

Multicolor Observations of Phobos with the Viking Lander Cameras: Evidence for a Carbonaceous Chondritic Composition

Abstract. *The reflectivity of Phobos has been determined in the spectral region from 0.4 to 1.1 micrometers from images taken with a Viking lander camera. The reflectivity curve is flat in this spectral interval and the geometric albedo equals 0.05 ± 0.01. These results, together with Phobos's reflectivity spectrum in the ultraviolet, are compared with laboratory spectra of carbonaceous chondrites and basalts. The spectra of carbonaceous chondrites are consistent with the observations, whereas the basalt spectra are not. These findings raise the possibility that Phobos may be a captured object rather than a natural satellite of Mars.*

Phobos, the inner moon of Mars, might have been created as part of the same event that gave birth to Mars or it may have formed elsewhere and subsequently been captured by Mars. The satellite's orbital characteristics provide some constraints upon hypotheses of its origin and early history (*1*). Additional clues may be provided by its composition.

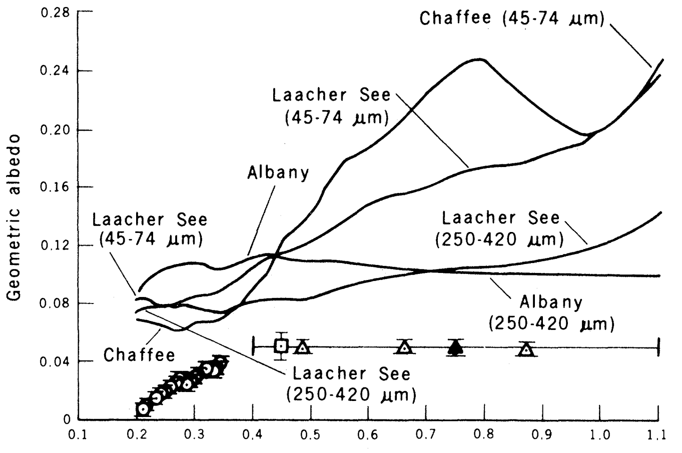

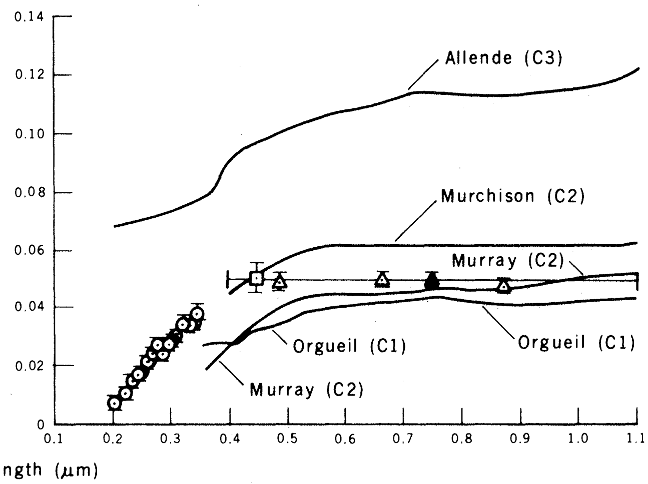

Fig. 1. Comparison between the observed reflectivity spectrum of Phobos and the measured behavior of a number of powdered basalts from Laacher See, Germany; Albany, Maine; and Chaffee County, Colorado. Open triangles, the closed triangle, the square, and circles refer to Viking narrow-band results, a Viking broad-band result, a ground-based photometric value, and Mariner 9 results, respectively. The reflectivity spectra of the basalt samples are shown as continuous lines and are labeled on the basis of their place of origin, with the numbers in parentheses giving the range of particle sizes present in the sample. Fig. 2. Comparison between the observed reflectivity spectrum of Phobos and the measured behavior of a number of powdered carbonaceous chondrite samples. Triangles, the square, and circles have the same meaning as in Fig. 1. The reflectivity spectra of the carbonaceous chondrite samples are shown as continuous lines and are labeled on the basis of their names, with symbols in parentheses giving the class of the sample. The spectral curves of the Allende and Murchison samples were obtained from the laboratory measurements reported here; that of the Murray and Orgueil samples came from (*8*). No attempt has been made to correct the reflectivity values of the latter to a phase angle of 0°. However, our laboratory studies suggest that these values should be increased by about a factor of 1.5. No such correction is needed for the other curves.

Spectral reflectivity measurements offer a useful means of remotely sensing the composition of the surfaces of bodies in the solar system. Because only a very limited range of the visible spectrum was covered (0.45 to 0.55 μm), past spacecraft and ground-based observations of Phobos have not led to a unique identification of its surface chemistry. However, these observations have greatly reduced the range of possibilities, with carbonaceous chondrites and basalts being the leading candidates among the materials that are abundant in the solar system (*2, 3*). To help resolve this compositional ambiguity, we have used a Viking lander camera to determine the reflectivity of Phobos in the spectral region from 0.4 to 1.1 μm, combined the results with measurements of the satellite's reflectivity in the region from 0.21 to 0.35 μm (*4*), and compared the composite spectrum with laboratory spectra of the compositional candidates.

On day 48 after landing at the second Viking site (23 October 1976), a sequence of 17 pictures of Phobos was obtained between 22:46 and 23:50 local lander time. Either two or three photographs were taken with each of six narrow-band channels as well as with a broadband survey diode. The narrow-band filters have half widths of about 0.1 μm, with effective wavelengths that range from about 0.49 to 0.87 μm (*5*). The survey diode is sensitive to light from about 0.4 to 1.1 μm (*5*). The instantaneous field of view of these diodes is 0.12°, which is somewhat smaller than the angular diameter of Phobos at the time of these observations (~ 0.17°). The instantaneous field of view was sampled every 0.04° so as to provide measurements of Phobos's brightness at a number of discrete positions.

We estimated the opacity of the martian atmosphere to light passing through it by comparing Phobos's brightness on pictures obtained at different elevation angles with a given diode. Additional information on atmospheric extinction was derived from a pair of sun pictures taken 4½ hours prior to the Phobos pictures. To determine Phobos's reflectivity in the spectral region from 0.4 to 1.1 μm from these pictures, we modeled the spatial response of the camera to an extended source, evaluated the disk-integrated brightnesses, removed from these values the effect of atmospheric extinction, and extrapolated these results to a phase angle of 0° for comparison with other data (*6*).

The open triangles in Figs. 1 and 2 show the values of Phobos's geometric albedo so obtained from pictures taken with the narrow-band blue, red, and IR2 diodes. The closed triangle refers to the albedo found from a picture taken with the broadband survey diode. The narrow-band points have been plotted at their effective wavelengths, and a horizontal line has been drawn through the broadband point to indicate the passband of the camera system for this diode. The vertical error bars attached to these data indicate an estimated relative error of ± 5 percent, due principally to uncertainties in the camera calibration. Relative error refers to the uncertainty in the shape of the reflectivity curve. The absolute error bar, estimated to be ± 20 percent, is due chiefly to a combination of uncertainties in the calibration and in the extinction correction. The average, absolute value for these four reflectivities of 0.05 ± 0.01 is consistent with a value of 0.06 ± 0.01 found from earlier observations at an effective wavelength of 0.55 μm (*3*).

Results from only four of the diodes are shown in Figs. 1 and 2 because we wished to define the shape of Phobos's reflectivity curve as accurately as possible. Since both the phase angle and the elevation angle changed appreciably over the entire sequence of pictures, it is important to choose pictures taken close together in time so as to minimize relative errors due to uncertainties in the atmospheric extinction, the dependence of brightness on phase angle, and the nonspherical shape of Phobos. Accordingly, we selected a consecutive sequence of blue, red, IR2, and survey pictures having the highest signal-to-noise ratio. Over the time period in which these pictures were taken, the phase angle changed by only 4° and the elevation angle by 0.4°. Pictures taken somewhat earlier with the other three diodes yielded albedos that agreed to 10 percent with those found from the later set.

Figures 1 and 2 also show albedos in the spectral region from 0.21 to 0.35 μm (circles) and an albedo at 0.45 μm (square). The former were found from an analysis of measurements made with the Mariner 9 ultraviolet spectrometer (*4*). The latter was derived from Kuiper's (*7*) ground-based photoelectric measurement of the ratio of Phobos's reflectivity at effective wavelengths of 0.45 and 0.55 μm. This observed ratio was multiplied by the Viking results near 0.55 μm to obtain a reflectivity value at 0.45 μm. The vertical bars on these results indicate the relative error.

A goniometer and a spectrometer (Cary 14) were used in tandem to obtain spectral reflectivity curves for powdered samples of basalts, carbonaceous chondrites, and several other materials. The goniometer spanned the spectral region from 0.397 to 1.223 μm, whereas the spectrometer covered the interval from 0.2 to 0.6 μm. Bidirectional reflectivity measurements were made with the goniometer, with the angles of incidence and view equal to 5° and 0°, respectively. The angle of incidence of the spectrometer was 45°, and reflected light was collected from all 4π steradians with an integrating sphere. Comparison of the two sets of data in their overlap region (from 0.4 to 0.6 μm) permitted an adjustment of the absolute scale of the spectrometer values to that of the goniometer values. Since only two samples of carbonaceous chondrites were available for these laboratory measurements, we supplemented their spectra with those for other specimens that were obtained over a more limited spectral region (*8*). The latter were measured with an instrument having a geometry similar to that of the Cary 14 spectrometer.

In Fig. 1, we compare the observed reflectivity behavior of Phobos with that of a number of basalt samples. In some cases, such as the Laacher See (45 to 74 μm) sample, the reflectivity declines markedly in the shorter wavelength portion of the spectrum. But, in conflict with the observations for Phobos, the reflectivity curves do not flatten at the longer wavelengths and the absolute values are much too high. In other cases, such as the Albany sample, the reflectivity curves are approximately flat at the longer wavelengths but they do not exhibit a sharp decline at the shorter wavelengths; moreover, the absolute values of these curves are somewhat too high.

Figure 2 shows the reflectivity curves for several samples of carbonaceous chondrites as well as the observed Phobos data. Lower subclass numbers mean that the sample has experienced less metamorphism. All the samples have relatively flat reflectivity spectra in the longer wavelength region, in approximate accord with the observations. Although the absolute values for the C1 and C2 samples are compatible with the observed value in this spectral interval, that of the C3 sample is not. Similar absolute values characterize many members of these subclasses, although there are a few exceptions (*8*). The reflectivity curves of the carbonaceous chondrites exhibit a wide dispersion in their reflectivity characteristics at shorter wavelengths, which range from the relatively shallow slope of the Orgueil sample to the steep decline of the Murray sample. This range in ultraviolet shapes overlaps the shape of the observed curve.

We also have compared the reflectivity spectra of ordinary chondrite meteorites, an enstatite meteorite, and the mineral magnetite with that of Phobos. None of these materials gave a satisfactory match to the observed data. Thus, the spectral characteristics of carbonaceous chondrites, especially those belonging to subclasses C1 and C2, are consistent with those of Phobos but the spectral characteristics of basalts and several other materials are not. We do not claim a unique identification on the basis of these comparisons. However, we have tried to include candidate substances that are abundant in the solar system and that have a low visible albedo.

The above analysis indicates that the spectral signature of Phobos at ultraviolet, visible, and near-infrared wavelengths is dominated by carbonaceous chondritic material. This finding is reinforced by a similar conclusion reached by Pang *et al.* (*4*) from a comparison of the combined Viking–Mariner 9 spectrum of Phobos with that of other bodies in the solar system. By analogy to the moon (*9*), meteoroidal material should constitute only a minor fraction of the topsoil of Phobos and thus our compositional results apply to the intrinsic surface of Phobos. Since Phobos is a tiny object (~ 20 km in diameter) and its surface is composed of a nonigneous material, carbonaceous chondritic material probably makes up its bulk composition as well as its surface composition (*4*).

A bulk density of 2.0 ± 0.6 g/cm^3 has been found for Phobos from Viking orbiter data (*10*). This result provides independent evidence that Phobos is made of carbonaceous chondritic material and also indicates that it may be made of the most volatile-rich and most primitive type of carbonaceous chondrite (class C1) (*10*).

Our compositional results have some implications for the origin of Phobos. In recent years, the "natural satellite" hypothesis has been the most popular one, principally because of Phobos's orbital characteristics (*1, 2*). It has seemed that tidal interactions represented the only plausible way for Mars to capture Phobos (*1*). Intricate scenarios can be devised by which such a tidal capture can occur and can lead to a present state consistent with the observed one (*11*). However, more straightforward tidal capture models imply that the capture of an object as small as Phobos is extremely improbable and that time scales greatly in excess of the age of the solar system are required for the orbit of such an object to evolve to one having its observed low eccentricity and low inclination (*1, 11*).

The compositional results of this report may force a reevaluation of the natural satellite hypothesis of Phobos's origin. Visible and near-infrared spectral studies of the brighter asteroids indicate that carbonaceous chondrites are found preferentially in the outer portion of the asteroid belt (*12*). Furthermore, according to some compositional models for the formation of bodies of the solar system (*13*), temperatures in the primordial solar nebula may have been too high for carbonaceous chondritic material, especially of the volatile-rich subclasses C1 and C2, to be made at the distance of Mars from the sun. Although these arguments are by no means definitive, they may add some support to the capture hypothesis.

The problems inherent in accounting for the origin of Phobos according to the tidal capture hypothesis may be overcome through consideration of an alternative capture mechanism. Recent calculations indicate that gas drag by Jupiter's primordial nebula may have led to the capture of Jupiter's outer, irregular satellites (*14*). This mechanism may also have relevance for the capture of Phobos in the early history of the solar system, at a time when Mars may also have had an extended gaseous envelope (*14, 15*).

JAMES B. POLLACK
Theoretical and Planetary Studies
Branch, NASA Ames Research Center,
Moffett Field, California 94035
JOSEPH VEVERKA
Laboratory for Planetary Studies,
Cornell University,
Ithaca, New York 14853
KEVIN PANG
Planetary Science Institute,
Pasadena, California 91101
DAVID COLBURN
Theoretical and Planetary Studies
Branch, NASA Ames Research Center
ARTHUR L. LANE, JOSEPH M. AJELLO
Jet Propulsion Laboratory, California
Institute of Technology, Pasadena 91103

References and Notes

1. J. A. Burns, *Rev. Geophys. Space Phys.* **10**, 463 (1972).
2. J. B. Pollack, J. Veverka, M. Noland, C. Sagan, T. C. Duxbury, C. H. Acton, Jr., G. H. Born, W. K. Hartmann, B. A. Smith, *J. Geophys. Res.* **78**, 4313 (1973).
3. B. H. Zellner and R. C. Capen, *Icarus* **23**, 437 (1974).
4. K. D. Pang, J. B. Pollack, J. Veverka, A. L. Lane, J. M. Ajello, *Science* **199**, 64 (1978).
5. F. O. Huck, H. F. McCall, W. R. Patterson, G. R. Taylor, *Space Sci. Instrum.* **1**, 189 (1975).
6. J. B. Pollack, D. Colburn, R. Kahn, J. Hunter, W. Van Camp, C. W. Carlston, M. R. Wolfe, *J. Geophys. Res.* **82**, 4479 (1977).
7. G. P. Kuiper as quoted by D. L. Harris, in *Planets and Satellites*, G. P. Kuiper and B. M. Middlehurst, Eds. (Univ. of Chicago Press, Chicago, 1961), p. 272.
8. M. J. Gaffey, *J. Geophys. Res.* **81**, 905 (1976).
9. J. Gros *et al.*, in *Proceedings of the Seventh Lunar Science Conference* (Pergamon, New York, 1976), p. 2403.
10. R. H. Tolson *et al.*, *Science* **199**, 61 (1978).
11. S. F. Singer, in *The Physical Studies of Minor Planets*, T. Gehrels, Ed. (NASA publication SP-267, National Aeronautics and Space Administration, Washington, D.C., 1971).
12. C. R. Chapman, D. Morrison, B. Zellner, *Icarus* **25**, 104 (1975); D. Morrison, *ibid.* **31**, 185 (1977).
13. J. S. Lewis, *Earth Planet. Sci. Lett.* **15**, 286 (1972); *Science* **186**, 440 (1974).
14. J. B. Pollack, J. Burns, M. Tauber, *Bull. Am. Astron. Soc.* **9**, 455 (1977).
15. D. Hunten, personal communication.
16. We thank the members of the Viking lander imaging team for their help in obtaining the photographs of Phobos, R. Kahn for his help in planning the pictures, and B. Baldwin for her aid in preparing the figures.

6 June 1977; revised 20 September 1977

Genetic Defect in Biosynthesis of the Precursor Form of the Fourth Component of Complement

Abstract. *Under cell-free conditions, liver polysomes from guinea pigs genetically deficient in the fourth component of complement (C4) did not synthesize pro-C4 (the precursor of C4), but did synthesize nascent C4 polypeptides which remained polysome bound. The defect was specific for pro-C4 synthesis since the amounts of total protein and albumin synthesis and release from C4-deficient polysomes were similar to that in normal guinea pig liver polysomes.*

Complement, a group of 19 plasma proteins, is one of the principal humoral effectors of inflammatory reactions. A deficiency of the fourth component of complement (C4) in guinea pigs, described by Ellman *et al.* (*1*), is inherited as an autosomal recessive trait and is genetically linked to histocompatibility loci (*2*). No C4 protein is found in serums from homozygous-deficient animals even with the use of sensitive methods capable of detecting one-millionth the normal levels of C4 (*3*). Cells and tissues from homozygous C4-deficient animals neither synthesize nor secrete C4 in vitro under conditions that support synthesis by normal cells (*4*). Somatic cell hybrids of C4-deficient peritoneal macrophages from guinea pigs with (human) HeLa cells synthesize C4 of human origin (*5*), although neither parent cell alone produces C4. A factor has been isolated from guinea pig peritoneal macrophages which is capable of inducing HeLa cells to synthesize and secrete C4 (*6*). The factor is present in C4-deficient macrophages at concentrations at least five times greater than that in normal macrophages. In order to investigate further the molecular basis for genetic control of C4 synthesis, we designed a cell-free protein synthesizing system (*7*). We now find, using this method, evidence for a defect in specific C4 messenger RNA (mRNA) translation on polysomes from homozygous C4-deficient guinea pigs.

Polysome preparations from a homogenate of normal guinea pig liver (S-20) (*8*) were incubated in the presence of radioactively labeled amino acids and an energy-generating system under optimal ionic conditions (*7*). Radioactively labeled C4 was detected by immunoprecipitation with C4 carrier protein and antiserum to guinea pig C4. Equivalent amounts of bovine gamma globulin (BGG) and antiserum to BGG or ovalbumin (OVA) and antiserum to OVA immunoprecipitates served as controls for nonspecific precipitation of radioactivity. Labeled guinea pig albumin was assayed in a similar manner with the use of guinea pig albumin (GPA) carrier protein and antiserum to GPA; controls consisted of equivalent precipitates of porcine albumin and antiserum to porcine albumin. In an earlier study, analysis of immunoprecipitates on sodium dodecyl sulfate (SDS) polyacrylamide gels indicated that C4 is synthesized as a single polypeptide chain precursor protein, designated pro-C4 (*7*), which is then converted to the three-chain structure (molecular weights of 95,000, 78,000, and 31,000) characteristic of serum C4 (*9*).

With these methods, the protein synthesizing capacities of normal and C4-deficient polysomes were compared. Polysomes from normal guinea pig liver and, in a separate reaction mixture, polysomes from homozygous C4-deficient guinea pigs were incubated for 90 minutes under optimal conditions for cell-free protein synthesis (*7, 8*). Polysomes were removed by centrifugation at 100,000*g* for 2 hours, and the released proteins were assayed for pro-C4 and GPA by immunoprecipitation. Control immunoprecipitates were also formed, and the radioactivity nonspecifically precipitated was compared to that in antiserum to C4 and antiserum to GPA precipitates. Total protein synthesis as assessed by precipitation of radioactivity with hot trichloroacetic acid (TCA) was similar in each. About 50 percent of the synthesized protein was released from polysomes, 3 to 4 percent of which was GPA and about 0.2 percent pro-C4. For C4-deficient polysomes, radioactivity specifically precipitated by antiserum to C4 was similar to control immunoprecipitates (Fig. 1). Analysis of the immunoprecipitates by means of electrophoresis on SDS-polyacrylamide gel (Fig. 1) showed synthesis and release of pro-C4 by normal polysomes, but no pro-C4 in the polysome-free supernatant from C4-

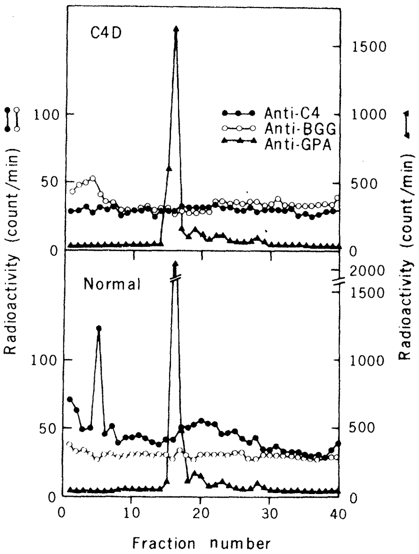

Fig. 1. Cell-free synthesis and release of pro-C4 and albumin by polysomes from homozygous C4-deficient (*C4D*) and normal guinea pig liver (*8*). Immunoprecipitable radioactivity was determined by electrophoresis on 1 percent SDS-polyacrylamide gel (5.6 percent) containing dithiothreitol (50 mM). Total and immunoprecipitable radioactivity (before application to the gels) is expressed as counts per minute per 100 μl. Normal: total protein (TCA precipitate), 1.69×10^6; released from polysomes (TCA precipitate), 9.4×10^5; albumin, 4.12×10^4; C4, 3.49×10^3; BGG control, 1.68×10^3; porcine albumin control, 2.68×10^3. C4-deficient: total protein (TCA precipitate), 2.41×10^6; released from polysomes, 1.20×10^6; albumin, 3.56×10^4; C4, 1.12×10^3; BGG control, 1.00×10^3; porcine albumin control, 4.02×10^3. This experiment was repeated more than 12 times with normal S-20 and four times with homozygous C4-deficient S-20. In the normal S-20, radioactivity in the pro-C4 ranged from 100 to 2500 count/min (see also Fig. 2); no pro-C4 was detected in any of the C4-deficient S-20 preparations.